Combined experimental and simulation studies of crosslinked polymer brushes under shear

Article

Accepted Version

It is advisable to refer to the publisher's version if you intend to cite from the work. See Guidance on citing.

www.reading.ac.uk/centaur

Combined Experimental and Simulation Studies of Crosslinked Polymer Brushes under Shear

Manjesh K. Singh[1**], Chengjun Kang[2**], Patrick Ilg[3],

Rowena Crockett[4], Martin Kröger[5], Nicholas D. Spencer[6*]

[1]Polymer Theory, Max Planck Institute for Polymer Research, D-55128 Mainz, Germany.

[2]Institute of Chemistry and Biotechnology, Zurich University of Applied Sciences, CH-8820 Wädenswil, Switzerland.

[3]School of Mathematical, Physical and Computational Sciences, University of Reading, Reading RG6 6AX, United Kingdom.

[4]Swiss Federal Laboratories for Materials Science and Technology, Empa, CH-8600 Dübendorf, Switzerland

[5]Polymer Physics, Department of Materials, ETH Zurich, CH-8093 Zurich, Switzerland.

[6]Laboratory for Surface Science and Technology, Department of Materials, ETH Zurich, CH-8093 Zurich, Switzerland.

ABSTRACT: We have studied the effect of crosslinking on the tribological behavior of polymer brushes using a combined experimental and theoretical approach. Tribological and indentation measurements on poly(glycidyl methacrylate) brushes and gels in the presence of dimethylformamide solvent were obtained by means of atomic force microscopy. To complement experiments, we have performed corresponding molecular-dynamics (MD) simulations of a generic bead-spring model in the presence of explicit solvent and crosslinkers. Our study shows that crosslinking leads to an increase in friction between polymer brushes and a counter-surface. The coefficient of friction increases with increasing degree of crosslinking and decreases with increasing length of the crosslinker chains. We find that the brush-forming polymer chains in the outer layer play a significant role in reducing friction at the interface.

[**]This work was carried out at the Laboratory for Surface Science and Technology, Department of Materials, ETH Zurich, 8093 Zurich, Switzerland.

1 Introduction

Crosslinked polymer brushes are often referred to as polymer brush-gels or simply gels. These polymer gels can swell either in water (hydrogels) or oil (lipogels)[1] making them highly suitable candidates for applications in the fields of drug delivery, pharmaceuticals, tissue engineering and other bio-medical applications[2-5]. Surface-grafted polymer gels can be prepared using two different methods (i) in situ and (ii) ex situ. In the in situ method, the polymer gels are prepared by crosslinking the chains while growing them from the grafting surface, whereas in the ex situ method, polymer gels are prepared by crosslinking the chains in a subsequent step.

Polymer brushes have long been studied using experimental[6-9], theoretical[10-14] and modeling[15-21] approaches. Polymer-brush-bearing surfaces exhibit very low friction in a good solvent[8,22,23]. Strong repulsive forces of entropic origin largely prevent the interpenetration of polymer chains grafted on opposing surfaces. Such forces lead to the formation of a thin fluid film between opposing brushes that assists in reducing friction[7]. Studies have been carried out to study the effect of different design parameters, such as molecular weight or chain length[24-27], grafting density[21,28-31], chain-stiffness[29] and solvent quality[8,32-34] on the tribological behavior of polymer brushes.

There has also been interest in studying the effect of crosslinking on the shear response of polymer brushes.[4,35-42] Lin et al.[43] investigated the effect of crosslinking density and stiffness on the macroscopic behavior of a type 1 collagen gel. It was found that an increase in the crosslinking density and stiffness (of crosslinkers) leads to an increase in the stiffness of the gel but the crosslinking density plays the dominant role. The grafted

poly[styrene-b-(ethylene-co-butylene)-b-styrene] (SEBS) gel layer showed improved tribological properties (less wear and lower friction coefficient) in comparison to the dry grafted SEBS layer and an n-octadecyltricholorosilane self-assembled monolayer[44]. Recently, the effect of crosslinking was studied using pentaerythritol tetra-acrylate as a crosslinking agent for polyethylene oxide gels[45]. It was found that an increase in crosslinker concentration lowers the swelling ratio and increases tensile stress. Crosslinking is known to improve the wear behavior of polymer brushes[35,46,47]. Kobayashi et al[48] recently showed that the macroscopic friction properties of a diamond-like-carbon-silicon (DLC-Si) specimen can be significantly improved by fabrication of an oleophilic cross-linked copolymer brush layer on its surface. Pan et al.[38] studied the friction properties of poly(vinyl alcohol) hydrogels against titanium alloys for biotribological applications under varying loads and shear speeds. They concluded that the effect of load on friction was more significant than that of the speed. Poly(2-hydroxyethyl methacrylate) (PHEMA) hydrogels have been of particular interest to researchers for their potential biotribological applications, and studies have been carried out for different combinations of substrate and counter-surface.[4,37,49,50] Li et al.[35] studied the effect of degree of crosslinking on the mechanical and tribological behavior of poly(acrylamide) (PAAM) brushes and hydrogels. They found that covalently crosslinked hydrogels display higher Young's moduli and coefficients of friction in comparison with surface-grafted polymer brushes and the effect was found to increase with the degree of crosslinking. In contrast, Ishikawa et al.[51] compared the effect of mechanical properties and of chemical characteristics (polymer hydration) on

tribological behavior of hydrogels via pin-on disk experiments, and concluded that the chemical characteristics (e.g. hydration) were the dominant factors. Ohsedo et al.[50] studied the effect of the presence of well-defined polymer brushes on gel surfaces. Their study showed that longer poly(sodium 4-styrenesulfonate) (PNaSS) brushes on PHEMA gels exhibit lower friction at low sliding speeds. Dunn et al.[3] explored the distinction between a self-mated "gemini" hydrogel interface and hydrogels sliding against hard, impermeable counter-surfaces and demonstrated that Gemini interfaces have very low friction coefficients, which are independent of sliding speed. On the other hand, hydrogels sliding against rigid impermeable surfaces exhibit higher friction, which is strongly dependent on sliding speed or time in contact. Thus, experimental studies have mainly focused on the role of solvent and effect of degree of crosslinking on the tribological behavior of gels but to the best of our knowledge the role of the length of crosslinkers has not yet been studied in detail.

We carried out complementary experimental and simulation studies to understand the tribological behavior of polymer brushes and gels. We characterized the tribological behavior of poly(glycidyl methacrylate) (PGMA) brushes and gel systems using a colloidal-probe-based lateral force microscopy (LFM) technique. Friction measurements were carried out at various applied loads, while maintaining the sliding speed constant. Polymer brushes and gels were modeled using a multibead-spring, coarse-grained molecular-dynamics simulation technique. We are going to compare the experimental outcome with modeling results to rationalize the effect of crosslinker chains on the frictional behavior of polymer brush-gels.
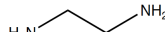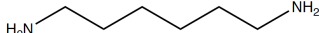
2 Methodology

2.1 Experiment

2.1.1 Materials

Friction experiments were performed on PGMA brushes and gels in dimethylformamide (DMF). The polymers were synthesized using the surface-initiated atom-transfer radical polymerization[52] (SI-ATRP) method on a silicon surface. They are characterized by their mean molecular weight M_n = 281.7 x 10^3 gm/mol and a polydispersity index PDI = 1.4. The grafting density of the polymer brushes and gels is $\rho_{expt} \approx 0.16/nm^2$, i.e., 50 times the critical grafting density[21], $\rho^* = (\pi R_g^2)^{-1}$. For details about the estimation of these characteristics for our polymer brushes and gels, see Supplementary Information SI.

The typical procedures for SI-ATRP of glycidyl methacrylate (GMA) were as follows: 0.141g (0.9 mmol) bipyridine (bpy) were dissolved in a mixture of 5 ml GMA (0.037mol), 1ml H_2O and 4ml methanol. The mixture underwent four freeze-pump-thaw circles (15 min each) to remove dissolved oxygen. In the next step the mixture was transferred to another flask containing 52.8 mg CuBr (0.37 mmol) and 4.5 mg $CuBr_2$ (0.02 mmol). After stirring for 10 min at room temperature, the mixture was immediately transferred to freshly prepared, initiator-modified silicon substrates. Polymerization was carried out at room temperature for various lengths of time without stirring, after which the silicon substrates were removed from the polymerization solution and sonicated in DMF to remove weakly adsorbed polymer. PGMA brushes were cross-linked by ethane-1,2-diamine or ethane-1,6-diamine in a post-modification manner. Amines can, in principle react with the epoxypropyl groups in the PGMA in several different ways, since an

amine can react with one, two, or even three epoxypropyl groups, and each end of the crosslinker could react with a different number. However, after a series of experiments (detailed in the SI), it was determined that under the conditions used, each end of each crosslinker reacted with a single epoxypropyl group.

Table 1: Table summarizing experimental brushes and gels under study, and in particular the crosslinkers used in preparing PGMA gels.

Materials			Degree of Crosslinking	Dry Thickness
PGMA Brushes			——	93 nm
PGMA gels	H_2N⌒NH_2 ethane-1,2-diamine **Crosslinkers C_2**		5 %	94 nm
			15 %	96 nm
			50 %	102 nm
	H_2N〰NH_2 hexane-1,6-diamine **Crosslinkers C_6**		3 %	94.5 nm
			18 %	100 nm
			36 %	107 nm

Details of polymer brushes and gels used in the tribological experiments are presented in Table 1. Dry thicknesses of PGMA brushes and gels were measured with a variable-angle spectroscopic ellipsometer (VASE, M-2000F, LOT Oriel GmbH, Darmstadt, Germany) at an incident angle of 70°, using a three-layer model (software WVASE32, LOT Oriel GmbH, Darmstadt, Germany), each sample being measured at three different spots. Crosslinkers of two different lengths were used to prepare PGMA gels with different degrees of crosslinking, to facilitate the study of the effect of length and

degree of crosslinking on the tribological behavior of the gels. By degree of crosslinking (*p*) we mean,

$$p = \frac{2 \times \text{number of crosslinkers}}{\text{number of polymer chains} \times \text{degree of polymerization}} \times 100\,\% \qquad (1)$$

2.1.2 Methods

Frictional and normal forces between a silica microsphere and PGMA brushes/gels were measured in the presence of DMF solvent by means of atomic force microscopy (AFM). All the measurements were performed using the MFP 3D Instrument (Asylum Inc., Santa Barbara, USA). Asymmetric contact (i.e. brush/gel against bare microsphere) was used, in order to obtain a measurable friction value, because friction in symmetric contact (brush-against-brush contact system) is so low as to be at the limit of the resolution of LFM measurements.

The AFM was operated in contact mode, the lateral and normal movements of the cantilever being monitored with a laser beam, reflected off the rear of cantilever and detected with a 4-quadrant photo-diode. These normal and lateral movements of the cantilever can be quantitatively related to the normal and lateral forces acting between the cantilever-tip and sample surface if the stiffness of the cantilever and sensitivity of the photo detector with respect to the cantilever position in the respective direction are known.

A non-destructive calibration procedure, the thermal-noise method[53], was used to estimate the normal stiffness of NSC36 (MicrosMasch, Tallinn, Estonia) cantilever.

Sader's method[54] was used to calibrate the torsional spring constant of the cantilever. A home-built micromanipulator (attached to a BX 41, Olympus optical microscope, Japan) was used to attach the colloid particles to a tipless cantilever. In the current study, silica microspheres (Kromasil, EKA Chemicals, Sweden) with a diameter, d = 14 μm (for the friction experiment) or d = 10 μm (for the indentation experiment) were attached to different tip-less cantilevers using a UV-curable glue (NOA 61, Norland Optical adhesive, Cranbury, NJ) and were cured overnight using a UV lamp (9W, Panacol-E losol). The lateral sensitivity, S_L of the AFM cantilever was estimated using the 'test-probe' method[55] as described by Cannara et al. In this method, a colloidal sphere is attached to the cantilever used for calibration, referred to as the 'test-cantilever'. The 'test-cantilever' is of similar width and thickness as the cantilever used for measurements or the 'target-cantilever'. The diameter of the colloidal sphere, d = 80 μm used for the test cantilever is larger than the width of the cantilever.

For lateral-force measurements, 10 'friction-loops' along the same line were acquired at each load. A scanning rate (n) of 1.0 Hz and stroke length (a) of 0.5 μm were used. Thus, the shear speed applied was calculated as $v = 2na$ = 1 μm/sec. Both the average friction force and the standard deviation were calculated. All the friction experiments were carried out at room temperature (T = 300 K).

2.2 Simulation

We investigated an explicit solvent-based multibead-spring generic coarse-grained model by means of MD simulation. Chains were permanently grafted by one end to a planar surface. To ensure that beads do not cross the grafting surface, an additional 9/3

repulsive wall potential U_{wall} was used with cut-off $z_c = 0.5\sigma$. Each grafted chain within

the polymer brush consisted of N Lennard-Jones (LJ) beads, linearly interconnected by

finite extendable nonlinear elastic (FENE) springs. Each chain was attached to the

substrate by one of its ends using an immobile tether bead (red beads in Fig. 1). The rest

of the beads in each chain were free to move and interact with other polymer beads,

the solvent, and the repulsive walls, confining the system to infinitely extended parallel-

plate geometry. The solvent was modeled as a simple fluid using spherical beads (brown

beads in Fig. 1). A solvent molecule consists of one bead that has the same Lennard-

Jones diameter as a polymer bead. All the simulations were performed for the brush-

against-wall system. The wall was modeled with the help of frozen arrays of repulsive LJ

beads. The interaction potential of counter-wall/surface with solvent and polymer beads

in the simulation is not purely repulsive. We have used a LJ/12-6 potential with cut-off

$R_c = 2.5$ and $\epsilon = 1.0$. Periodic boundary conditions were applied only along the lateral

direction (along the x and y axis of Fig 1a), which coincides with the direction of sliding.

To be specific, the explicit solvent model was that employed earlier by Soddemann et

al.[56] and Dimitrov et al.[32] The Lennard-Jones (LJ/12-6) potential was truncated at its

minimum and shifted to some desired depth (polymer-polymer, solvent-solvent and

polymer-solvent energies ϵ_{pp}, ϵ_{ss} and ϵ_{ps}), continuing from its minimum to zero with a

potential having a cosine form and thus providing a potential that is both continuous

and has a continuous derivative at the cut-off distance $r_{c,in}$. The parameters $\epsilon_{pp} = \epsilon_{ss} =$

0 and $\epsilon_{ps} = 0.4$ were chosen to model good solvent conditions in the current work. We

have provided details of each potentials used in this work in Supplementary section SVI.
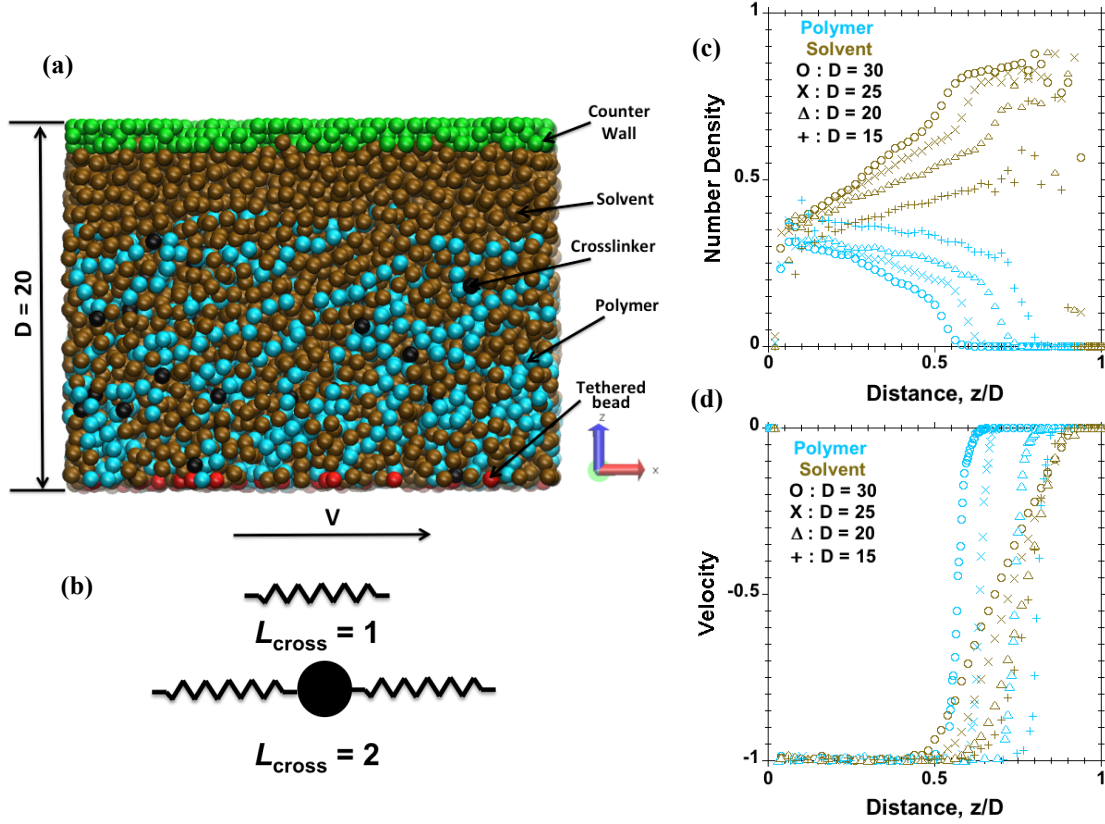
Figure 1: Representative information from the model brush-against-wall system with explicit solvent and crosslinkers, subjected to shear. (a) Snapshot, where polymer beads are colored cyan, tethered beads are colored red, solvent beads are colored brown and crosslinkers (L_{cross} = 2) are colored black, (b) schematic of crosslinkers of different lengths, (c) density profiles and (d) velocity profiles versus distance from the grafting surface (M = 50 chains tethered on the grafting surface, N = 50 beads per chain, grafting density, ρ = 0.075, length of crosslinkers, L_{cross} = 2 and number of crosslinkers, N_{cross} = 200 at velocity v = 1 applied on tethered beads.) All dimensional quantities are given in Lennard-Jones (LJ) units. This particular simulation was performed at very high shear velocity, v = 1, to achieve a visible amount of alignment, whereas the shear velocity of all subsequent simulations was taken as v = 0.001.

Temperature was kept constant by controlling the temperature of all the beads except for tethered and explicit wall beads, by explicitly rescaling their individual velocities[29,57]. We have used a profile-unbiased thermostatting (PUT) scheme. The velocity profile was calculated by computing the center-of-mass velocity of all beads residing in layers parallel to the grafting surface. The center-of-mass velocity of layers was used to define the 'bias-velocity', which was subtracted from the velocities of individual beads to

calculate their thermal velocities. These were rescaled to the desired value and subsequently the bias velocity was added. The temperature was maintained constant at $T = 1.2$ using a profile-unbiased thermostat as discussed above for all the simulation work in this manuscript.

Details for generating the crosslinked polymer brush were discussed in detail in our previous work[58]. For bonding within crosslinker chains and bonding between crosslinkers and polymer beads as part of the brush, we have used a harmonic bond potential,

$$E_H(r) = K_H(r - r_0)^2 \qquad (2)$$

Here K_H is the spring coefficient determining the bond stiffness, r_0 the equilibrium bond length and r is the distance between two bonded atoms at any given time. We have used $K_H = 100$ and $r_0 = 1$ to model rather stiff crosslinker bonds. The harmonic bond potential we use does not strictly prevent bond crossing, but bond crossing does not occur in practice for the chosen parameters, as described in the Supplementary Information SV. All simulated quantities reported in the current study are given in terms of LJ units[59]. The crosslinked polymer-brush system was generated for different numbers of crosslinkers (the number denoted by N_{cross}) with a fixed contour length of crosslinker (L_{cross}) chains and vice-versa. Figure 1b shows the explicit crosslinkers. $L_{cross} = 1$ for monomers of different chains bonded by crosslinker, while $L_{cross} = 2$ represents a single interior bead that is bonded to two beads in the respective chains to be crosslinked. The degrees of crosslinking (p) used in simulation work are $p = 0, 4, 8$ and 16

percentage, as defined in Equation 1. For our simulation, we have used LAMMPS (Large-scale Atomic/Molecular Massively Parallel Simulator)[60].

We have carried out simulations for the brush-against-wall model system described in Fig. 1. We note that the simulations have been performed at fixed separation distances D (while measuring load), whereas experiments are performed under prescribed normal load (implying a separation distance D). The simulations were performed on randomly grafted polymer chains on flat surfaces. The system consists of $M = 50$ chains on the tethering surface, while each linear chain is composed of $N = 50$ beads. As mentioned in the section 2.1.1 (see also Supplementary section SIII), the critical grafting density[21] for such polymer brush is $\rho^* = (\pi R_g^2)^{-1}$. We have considered grafting densities well within the brush regime, $\rho = 0.075$ (approximately $7\rho^*$). We have not considered additional bending stiffness of chains in the current work, i.e. the simulations were performed on flexible, excluded-volume chains. The total number of beads in the simulation box was such that the number density of beads was maintained at a typical value of approximately 0.8 at each separation between the grafting surface and counter wall.

3   Results and Discussion

3.1   PGMA Brushes and Gels in DMF

3.1.1 Colloidal-Probe Lateral Force Microscopy

The measured friction force as a function of normal load for PGMA gels with crosslinkers C_2 and C_6 at a shear velocity of 1 μm/sec is reported in Figs. 2a and 2b, respectively. These results are compared with the corresponding results for a bare silicon surface and PGMA brushes. The experiments were performed in DMF solvent using a tipless

cantilever of stiffness 0.976 N/m with a silica colloidal sphere of diameter 14 μm attached to it. The gels had different degrees of crosslinking. It can be seen that PGMA brushes on silicon surfaces in DMF reduce friction significantly when compared to bare silicon surfaces. The friction force was found to be higher for PGMA gels (i.e. with crosslinking) in comparison to PGMA brushes.

A monotonic increase in friction force is observed upon increasing the degree of crosslinking for gels with C_2 crosslinkers. At 5% degree of crosslinking the friction force is seen to remain close to that for uncrosslinked brushes. At 50% degree of crosslinking, the friction force is higher and even exceeds that of the bare silicon surface. The observed higher friction (in comparison to a bare silicon surface) can be attributed to an increase in contact area between the colloidal sphere and the gel.
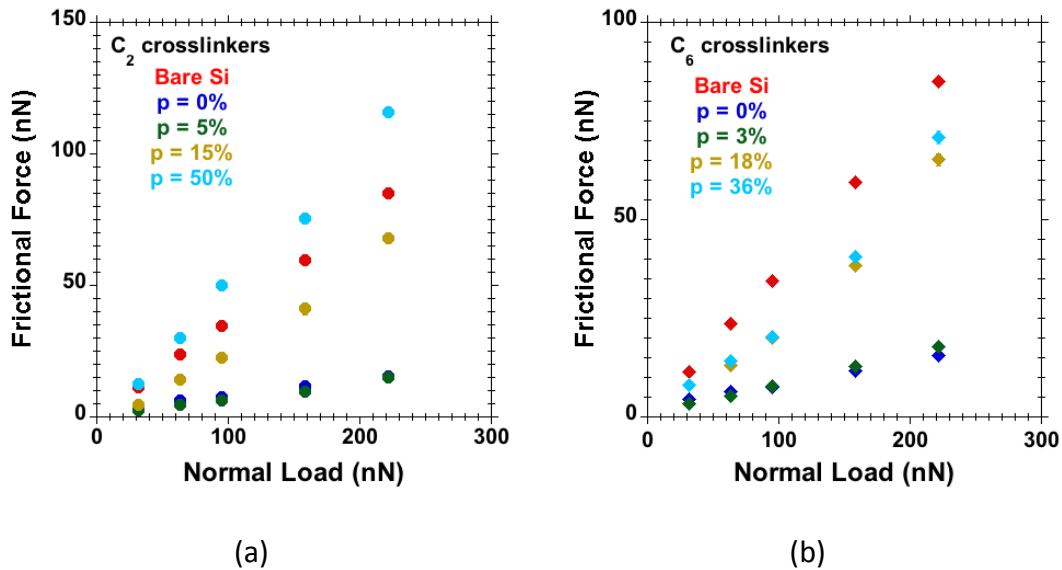

(a)   (b)

Figure 2: Friction force vs normal load for bare silicon surfaces and silicon surfaces bearing PGMA brushes and gels, measured by colloidal-probe lateral force microscopy experiments using a tipless cantilever (0.976 N/m stiffness) with an attached silica sphere of 14 μm diameter. PGMA gels have C_2 crosslinkers with a degree of crosslinking of 5%, 15% and 50%. The PGMA gels with C_6 crosslinkers have degrees of crosslinking of 3%, 18% and 36%. Experiments were performed at constant speeds of 1 μm/sec.

Friction is also found to increase with crosslinking degree for gels made with C_6 crosslinkers. At 3% degree of crosslinking, the friction force is only slightly larger than that measured on (non-crosslinked) PGMA brushes. At 18% degree of crosslinking, friction is notably greater than that on (non-crosslinked) PGMA brushes and PGMA gels with 3% degree of crosslinking. With a further increase in degree of crosslinking to 36%, no significant further increase in friction is observed compared to the results obtained with a 18% degree of crosslinking.

Similar experiments were carried out at a shear velocity of 5 µm/sec (Supplementary section SVII). A scanning rate (n) of 1.0 Hz and stroke length (a) of 2.5 µm were used. Thus, the shear speed applied was calculated as $v = 2na = 5$ µm/sec. The friction coefficient was found to increase with increasing shear speed for all the systems but the overall trend in terms of the effect of crosslinking was found to be very similar. Polymer brushes and gels in our experiments underwent sliding and were not simply deformed.

The friction force vs normal load curves show a linear relationship. The coefficient of friction can thus be extracted from the slope by linear-regression fitting. The obtained values for the coefficient of friction will be discussed in detail in section 3.3 of this manuscript.

3.1.2 Atomic-Force-Microscopy-Based Nanoindentation

AFM-based nanoindentation was employed to study the effect of crosslinking on the mechanical behavior of PGMA brushes and gels. The brushes and gels in DMF were indented with an AFM cantilever bearing a silica sphere of 10 µm diameter. The applied load (force) against penetration depth is presented in Fig. 3.
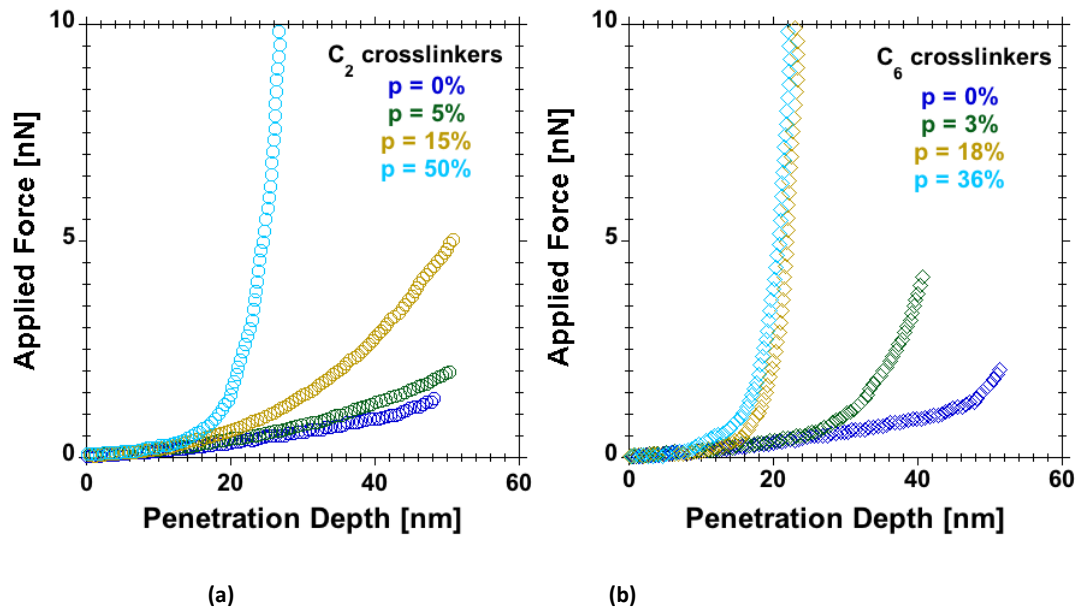
Figure 3: Applied force against penetration depth measured by colloidal-probe atomic force microscopy with a 10 µm silica sphere glued to a tipless cantilever (0.6 N/m stiffness). For (a) PGMA gels with C_2 crosslinkers and (b) PGMA gels with C_6 crosslinkers. % values denote the degree of crosslinking in each system (as for Fig. 2).

Figures 3a and 3b show the applied load against indentation depth for different PGMA gels with different crosslinking degrees for C_2 and C_6 crosslinkers respectively. A change in the slope of the force-vs-depth curve occurs at the depth where the AFM cantilever begins to be noticeably influenced by the substrate; the steep part is caused by a substrate effect (the substrate is close and the brush appears stiffer). In general, substrate influence begins to be felt at around 10% indentation of the unperturbed brush height[61,62]. Hence, we can approximate the height of the PGMA brushes and gels by the penetration depth before this sudden change of the indentation force. With C_2 crosslinkers, as the degree of crosslinking increases from 5% to 50% the substrate effect is shown at a lesser depth, which indicates a decrease in the swelling ratio with increase in degree of crosslinking. The indentation curves for PGMA brushes and PGMA gels with

5% crosslinking are similar, as are the friction forces measured by LFM, c.f. Fig. 2a. The plausible decrease in swelling ratio with an increase in the degree of crosslinking could explain the increase of friction force: with increasing in degree of crosslinking, there are few brush-forming chains available at the outer film layer, which are responsible for the low-friction behavior in polymer-brush based lubrication[9,23,35].

The indentation curves for PGMA gels with C_6 crosslinkers also reflect the tribological behavior of gels observed in LFM experiments. At a degree of crosslinking of 3%, the substrate effect is already significant at penetration depths above 30 nm (implying a decrease in swelling ratio compared to PGMA brushes), which correlates with the increase in coefficient of friction. As the degree of crosslinking is increased to 18%, there is a further decrease in swelling ratio, and an increase in coefficient of friction was observed (Fig. 2b). Upon further increasing the degree of crosslinking to 36% there is no significant change in the indentation behavior anymore; similarly we did not observe any significant change in the coefficient of friction.

3.2 MD Simulation

3.2.1 Equilibrium Molecular Dynamics Simulation

We equilibrated the polymer brush/gel against wall system at different separations D between the graft and the counter-wall surface (see Fig. 1a). A reduction of separation distance by 1 (LJ unit) was achieved as follows: A number of solvent beads were randomly removed from the system to ensure the same number density 0.8 at the new separation distance. The grafting surface was kept fixed and the counter-wall was

moved towards the grafting-surface with a constant velocity, v = 0.01 for a duration of 10^5 steps at an integration time step Δt = 0.001. At each separation D between the polymer-chain-bearing surface and counter-wall, the polymer-brush/gel system was allowed to equilibrate for 3×10^6 timesteps (10^6 steps at Δt = 0.001 followed by 2×10^6 steps at Δt = 0.0025).

Figure 4 shows the number-density profiles of polymer beads versus the z position measured from the grafting surface. Inspecting the density profiles, the systems with shorter crosslinkers show a decrease in brush height with increasing degree of crosslinking and more polymer density is accumulated at the grafting surface. There is hence a lower polymer concentration present towards the outer layer of grafted chains to assist in brush-mediated lubrication[9,63]. AFM-based indentation experiments (Fig. 3) show that the wet thickness decreases with increasing degree of crosslinking, the simulation observations are in complete agreement with the experiments.
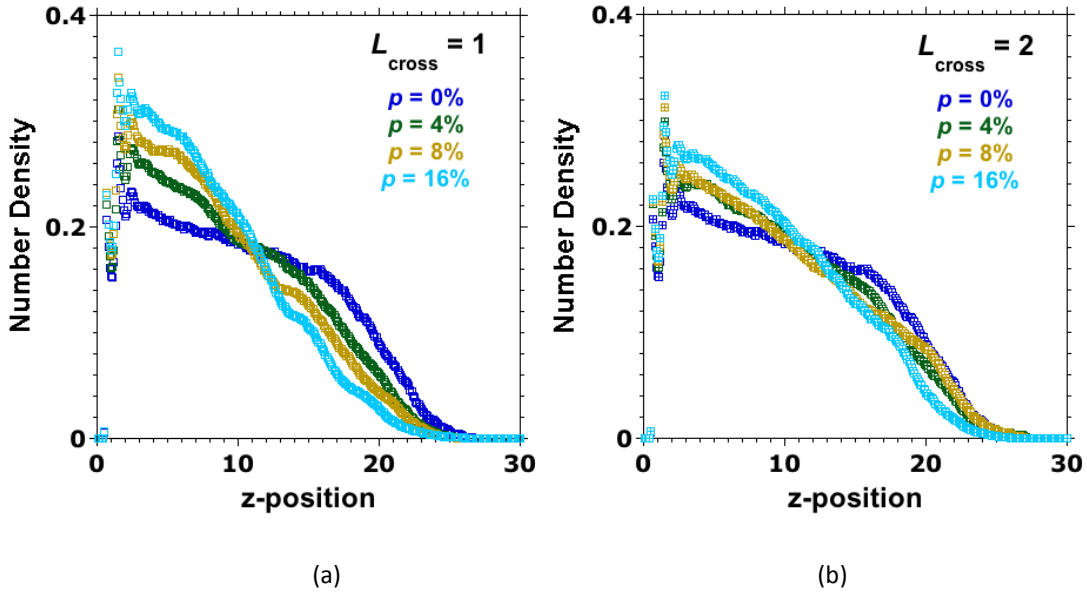
Figure 4: Density profiles for polymer brush/gel systems with M = 50, N = 50 and ρ = 0.075 in explicit solvent for a separation distance D = 30, having (a) L_{cross} = 1 and (b) L_{cross} = 2. Density profiles are shown for different degrees of crosslinking, p = 0, 4, 8 and 16 %.

3.2.2 Nonequilibrium Molecular Dynamics Simulation (NEMD)

The equilibrated systems at different separations (D) were used to run nonequilibrium MD (NEMD) simulations. Steady shear was applied by moving the tethered beads with the prescribed velocity, keeping the separation between walls constant during each run of given shear velocity[20,58]. At each separation and velocity, the stress tensor was calculated using the Irving-Kirkwood expression[59,64].

The NEMD studies were carried out at a fixed shear velocity, v = 0.001 applied on the tethered beads at different separations between explicit wall and polymer-bearing surface. At each separation, normal and shear stresses acting on the brush and crosslinkers were calculated for different combinations of lengths and numbers of crosslinkers, in order to study the effect of crosslinking on the frictional behavior of model polymer brushes. The simulations were done for 3×10^7 integration steps, where

18

data for the first 10^7 steps at timestep $\Delta t = 0.002$ were ignored to allow the system to reach steady state. Data for subsequent 2×10^7 steps at $\Delta t = 0.0025$ were recorded and analyzed. Simulations at each separation (D) were repeated for 10 different initial configurations of randomly grafted polymer chains and mean values from these runs are reported with error bars calculated from the corresponding standard deviations.

Figure 5 shows the results on the effect of degree of crosslinking on polymer brushes for different systems having crosslinkers of length $L_{cross} = 1$ and $L_{cross} = 2$. In particular, Figs. 5a and 5b display normal stress against distance curves for systems with $L_{cross} = 1$ and $L_{cross} = 2$ crosslinkers, respectively. It can be seen that the normal stress increases as the separation (D) between grafting-surface and counter wall-surface decreases for all the systems. For systems with $L_{cross} = 1$ crosslinkers the normal stress was found to be decreasing with increasing degree of crosslinking at all separations. The decrease in normal stress with the increase in the degree of crosslinking can be explained with the help of the density-profile curve (Fig. 4a). The brush height decreases with increasing degree of crosslinking; therefore less deformation is felt in brushes with a higher degree of crosslinking at the same separation between wall and the polymer-bearing surface. This results in a decrease of the normal stress at the same separation with increasing degree of crosslinking.
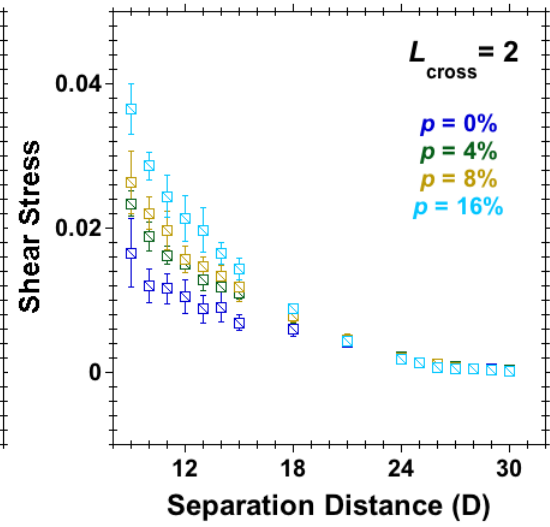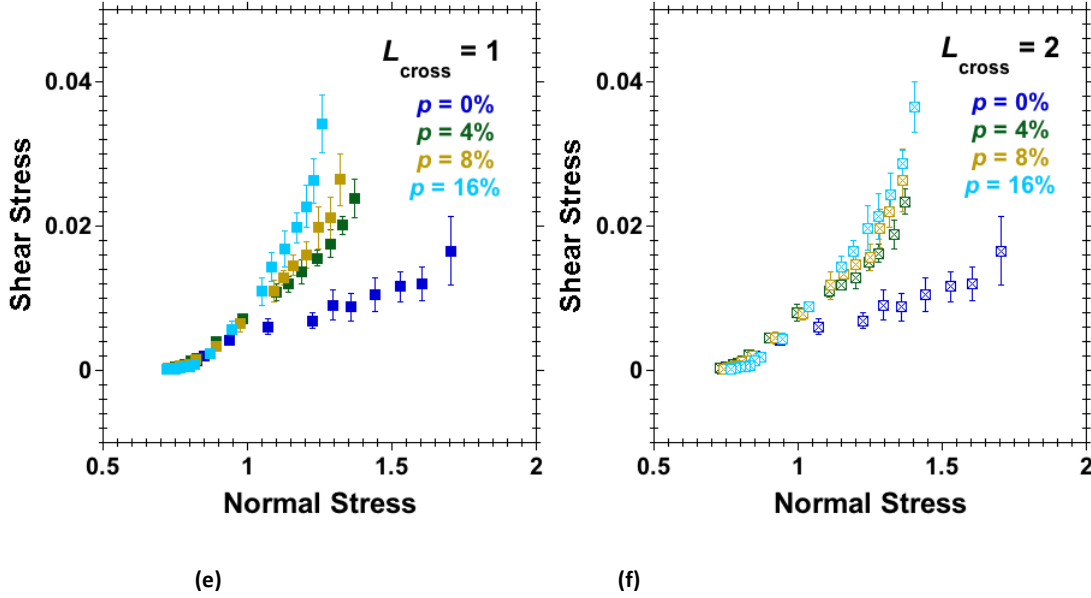
(a)

(b)

(c)

(d)

20
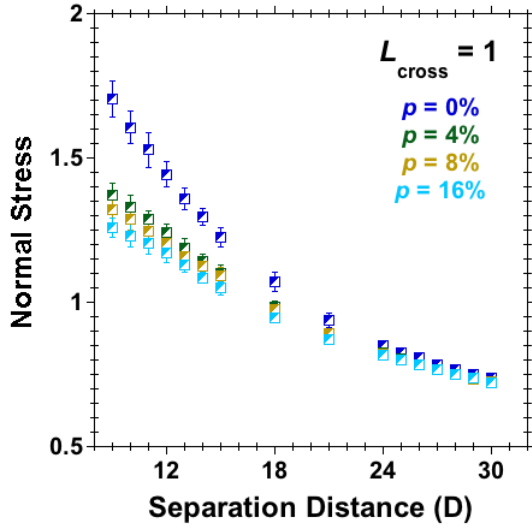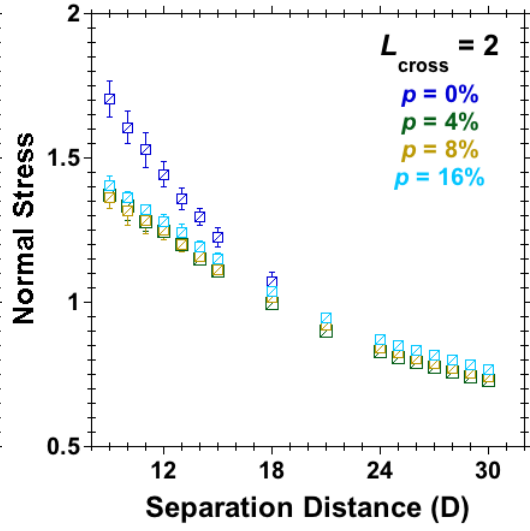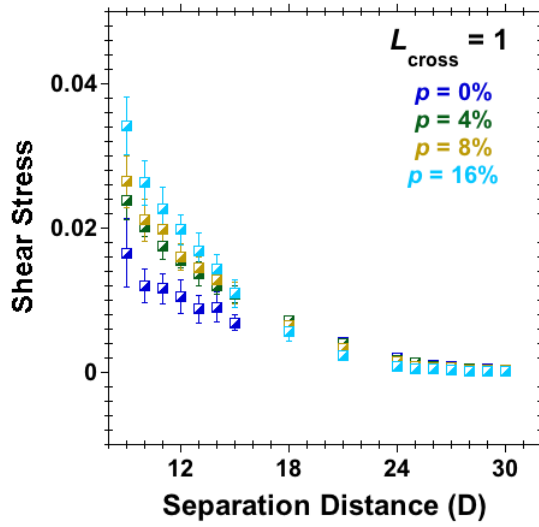
Figure 5: Simulated (NEMD) systems with $M = 50$, $N = 50$ and $\rho = 0.075$ in explicit solvent having different degrees of crosslinking, $p = 0, 4, 8$ and 16 %, (a)–(b): normal stress against separation, (c)–(d): shear stress against separation and (e)–(f): shear stress against normal stress each for systems having crosslinkers of length, $L_{cross} = 1$ and $L_{cross} = 2$ respectively.

For the system with $L_{cross} = 2$ crosslinkers, normal stress was found to be similar at different degree of crosslinking and lower in comparison to uncrosslinked system at all separations. This can be explained with similar density profiles for systems with different degrees of crosslinking. Figures 5c and 5d show the shear stress vs separation-distance for systems with $L_{cross} = 1$ and $L_{cross} = 2$ crosslinkers, respectively. We observe an increase in shear stress as the separation D between grafting-surface and counter wall-surface decreases for all the systems. We also notice an increase in shear stress with increasing degree of crosslinking at all separations. This increase in shear stress is found to be quite similar for $L_{cross} = 1$ and $L_{cross} = 2$. Figures 5e and 5f show a parametric plot of shear against normal stress for different separation distances D for systems with $L_{cross} = 1$ and $L_{cross} = 2$ crosslinkers, respectively. The shear stress for all the crosslinked systems

is found to be higher compared to that of the uncrosslinked system at a given normal stress. We also find an increase in shear stresses with increasing degree of crosslinking at all normal stresses for systems with L_{cross} = 1 and L_{cross} = 2 crosslinkers. These observations can be rationalized as follows. Crosslinking leads to an interdependent motion of crosslinked grafted chains under shear, resulting in an increase in the shear stress for all the crosslinked systems when compared to uncrosslinked polymer-brush systems. Under shear, the uncrosslinked systems are deformed more easily than a crosslinked network of polymer brushes.[36] The increase in the degree of crosslinking leads to more chains moving interdependently under shear. We therefore find an increase in friction upon increasing the degree of crosslinking.

3.3 Comparison between Simulation and Experimental Results

(a)   (b)
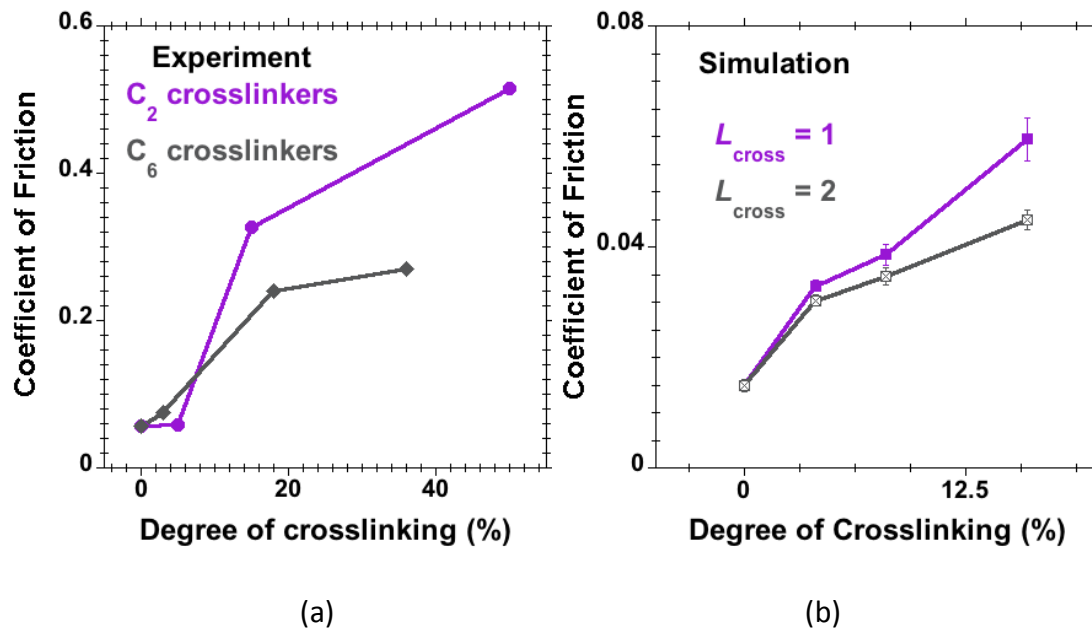
Figure 6: Coefficient of friction against degree of crosslinking for (a) Experimental results for systems with crosslinkers C_2 (brown lines) and C_6 (gray lines) at a shear speed of 1 µm/sec and (b) Simulation results for systems with M = 50 chains of length N = 50 for different lengths of crosslinkers, L_{cross} = 1 (pink lines) and L_{cross} = 2 (gray lines) at a shear speed, v = 0.001 for a brush-against-wall system.

We are now in a position to attempt a qualitative comparison of the experimental and simulation results. We compare these studies in terms of the coefficient of friction (CoF), which is a frequently used quantity to characterize the tribological behavior of surfaces (Fig. 6). To compare flow conditions between experiment and simulation the dimensionless Weissenberg number (Wi $= \dot{\gamma}\, \tau_{Rex}$ with shear rate $\dot{\gamma}$ and relaxation time τ_{Rex}) is typically used. Under the experimental and simulation conditions used in our study, Wi number have comparable values, as demonstrated in the Supplementary section SIV. Our simulations and experiments are located in the boundary-lubrication regime. Friction forces arise due to the interactions among wall, solvent and polymer beads. We have calculated the coefficient of friction from the slope of the friction force against normal force. Thus, the presented results for the coefficient of friction are unaffected by adhesion between wall and polymer brush. The interaction potential between wall and polymer beads in the simulation is not purely repulsive as mentioned already (section 2.2). It is important to note that the overall interaction between brush and wall can be considered repulsive. There is an attractive van der Waals force present between the brush and wall, which reduces the overall repulsion, but it does not lead to an overall attractive interaction. Van der Waals interactions between polymer brushes and surfaces are considered as "bridging forces" and can be specific or non-specific. Israelachvili[65] explained in detail various attractive "intersegment", "bridging" and "depletion" forces acting between polymers and counter surfaces. Under suitable conditions, "bridging forces" can lead to an overall attractive force.

For the experiments, a straight line was fitted to the friction force vs normal load curve in Fig. 2. The coefficient of friction is defined by the corresponding slope. Figure 6a shows the resulting CoF as a function of the degree of crosslinking measured by lateral force microscopy at a shear speed of $v = 1$ μm/sec for different lengths of crosslinkers. We see an increase in friction force with speed for both crosslinking lengths studied here which translates into an increase in CoF (not shown). We also find an increase in CoF with increasing degree of crosslinking (similar to Ref. 35) for both crosslinker lengths studied, while the CoF does not change significantly beyond a degree of crosslinking of 18% for C_6 crosslinkers. The coefficient of friction was found to be similar for C_2 and C_6 crosslinkers for lower degrees of crosslinking. At a higher degree of crosslinking, the friction was found to be lower for the gel with longer crosslinkers.

For the simulations, the coefficient of friction was estimated from the slope of the shear stress vs normal stress curves from the initiation of deformation ($D < 24$) of polymer brushes and gels. The shear stress vs normal stress curve in this regime is predominantly linear and a linear curve was fitted taking into account the error at each point in the curve[66]. Figure 6b shows the coefficient of friction vs the degree of crosslinking for different lengths of crosslinkers, as obtained from our simulations. In qualitative agreement with the experiments, the CoF for all the crosslinked systems is found to be higher than that of the uncrosslinked system. The coefficient of friction was also found to increase with the degree of crosslinking for systems having different lengths of crosslinkers in a very similar manner as observed in the experiments. Similar observations were made in the experimental results of Li et al.[35] where the coefficient of

24

friction was found to be increasing with increase in crosslinker content in PAAm hydrogel-brushes.

At sufficiently high degree of crosslinking, experiments and simulations both find that shorter crosslinker lengths lead to larger values of the CoF. This effect vanishes or is unclear at low degrees of crosslinking. The crosslinkers tend to restrict the configurational space for the chains, so that energetic effects become more relevant. This effect increases with decreasing crosslinker length and increasing degree of crosslinking. In the presence of crosslinkers, the brush thus adopts a more compact density profile (Fig. 4), which tends to resist sliding. As a result, the coefficient of friction increases with increasing degree of crosslinking.

4   Conclusions

Experimental and simulation studies were performed in order to clarify the effect of crosslinking on the tribological behavior of polymer brushes. The tribological experiments on PGMA brushes and gels in DMF solvent were performed against silica microspheres using the LFM technique. The PGMA brushes showed a remarkable decrease in friction forces when compared to bare silicon surfaces. We also observed a general increase in friction with crosslinking for PGMA brushes in DMF. An increase in the coefficient of friction was observed with increasing degree of crosslinking and a decreasing coefficient of friction was observed with increasing length of crosslinkers beyond a certain degree of crosslinking. AFM-based indentation of PGMA brushes and gels in DMF solvent showed a decrease in their swelling ratio with increasing degree of

crosslinking and can very well explain the tribological response of gels at different degrees of crosslinking for different lengths of crosslinkers.

Crosslinked polymer brushes were successfully modeled using the coarse-grained MD technique. The tribological behavior of crosslinked polymer brushes under shear has been qualitatively compared with that of uncrosslinked polymer brushes, and also with our experimental data. Simulations were performed at a constant shear velocity at different separations in the presence of explicit solvent beads. Results were presented in the form of shear stress vs normal stress. The coefficients of friction were calculated from the slopes of shear vs normal stress curves. The trends were consistent with the experimental observations: increase in coefficient of friction with increasing crosslinking degree and decrease in coefficient of friction with increasing crosslinker length. We were able to explain these findings with the help of simulated density profiles. As the degree of crosslinking increases, the polymer concentration in the outer layer that can participate in brush-assisted lubrication is reduced. In addition, crosslinked polymer brushes are more resistant to shear compared to their non-crosslinked counterparts. We did not attempt to match the shear speeds to achieve a better quantitative agreement between experiments and simulations. Rather, the present simulations aim to study the underlying effects seen in the experiments on a more qualitative level.

This work can be extended by performing studies over a wider range of degree of crosslinking for various lengths of crosslinkers to gain a better understanding of the influence of the length of crosslinkers on the mechanical behavior of gels under shear.

Acknowledgments

Associated Content

Supporting Information

The PDF file contains estimated characteristics of the experimentally studied polymer brushes, possible reaction routes between crosslinkers and polymer brushes, comparison of graft density between experiment and simulation, estimation of Weissenberg number under experimental and simulation conditions, possibility of bond crossing in harmonic bond used for crosslinking, potentials used in simulation, and friction force against normal load at speed 5 μm/sec. This material is available free of charge via the Internet at http://pubs.acs.org.

Author Information

Corresponding Author: *E-mail: nspencer@ethz.ch

Author Contributions: All authors contributed equally to this work. The draft has been prepared by M.K.S., and subsequently revised by all authors.

References

(1)   Richtering, W.; Saunders, B. R. Gel Architectures and Their Complexity. *Soft*

Matter **2014**, *10* (21), 3695–16.

(2)   Blum, M. M.; Ovaert, T. C. Investigation of Friction and Surface Degradation of Innovative Boundary Lubricant Functionalized Hydrogel Material for Use as Artificial Articular Cartilage. *Wear* **2013**, *301* (1-2), 201–209.

(3)   Dunn, A. C.; Sawyer, W. G.; Angelini, T. E. Gemini Interfaces in Aqueous Lubrication with Hydrogels. *Tribol. Lett.* **2014**, *54* (1), 59–66.

(4)   Freeman, M. E.; Furey, M. J.; Love, B. J.; Hampton, J. M. Friction, Wear, and Lubrication of Hydrogels as Synthetic Articular Cartilage. *Wear* **2000**, *241* (2), 129–135.

(5)   De Giglio, E.; Cafagna, D.; Giangregorio, M.; Domingos, M.; Mattioli-Belmonte, M.; Cometa, S. PHEMA-Based Thin Hydrogel Films for Biomedical Applications. J. Bioactive Compat. *Polym.* **2011**, *26* (4), 420–434.

(6)   Raviv, U.; Klein, J. Adhesion, Friction, and Lubrication Between Polymer-Bearing Surfaces. In *Polymer Science: A Comprehensive Reference;* Elsevier, **2012**; pp 607–628.

(7)   Klein, J.; Perahia, D.; Warburg, S. Forces Between Polymer-Bearing Surfaces Undergoing Shear. *Nature* **1991**, *352*, 143-145.

(8)   Nalam, P. C.; Ramakrishna, S. N.; Espinosa-Marzal, R. M.; Spencer, N. D. Exploring Lubrication Regimes at the Nanoscale: Nanotribological Characterization of Silica and Polymer Brushes in Viscous Solvents. *Langmuir* **2013**, *29* (32), 10149–10158.

(9)   Lee, S.; Spencer, N. D. Sweet, Hairy, Soft, and Slippery. *Science* **2008**, *319* (5863),

575–576.

(10)   Alexander, S. Adsorption of Chain Molecules with a Polar Head a Scaling Description. *J. Phys.-Paris* **1977**, *38* (8), 983–987.

(11)   De Gennes, P. G. Conformations of Polymers Attached to an Interface. *Macromolecules* **1980**, *13* (5), 1069–1075.

(12)   Milner, S. T.; Witten, T. A.; Cates, M. E. Theory of the Grafted Polymer Brush. *Macromolecules* **1988**, *21* (8), 2610–2619.

(13)   Zhulina, Y. B.; Pryamitsyn, V. A.; Borisov, O. V. Structure and Conformational Transitions in Grafted Polymer Chain Layers. a New Theory. *Polymer Science U.S.S.R.* **1989**, *31* (1), 205–216.

(14)   Semenov, A. N. Contribution to the Theory of Microphase Layering in Block-Copolymer Melts. *Zh. Eksp. Teor. Fiz.* **1985**, *25* (17), 1120–1121.

(15)   Kreer, T. Polymer-Brush Lubrication: a Review of Recent Theoretical Advances. *Soft Matter* **2016**, *12* (15), 3479–3501.

(16)   Grest, G. S. Computer Simulations of Shear and Friction Between Polymer Brushes. *Curr. Opin. Colloid Interf. Sci.* **1997**, *2* (3), 271–277.

(17)   Hoy, R. S.; Grest, G. S. Entanglements of an End-Grafted Polymer Brush in a Polymeric Matrix. *Macromolecules* **2007**, *40* (23), 8389–8395.

(18)   Grest, G. Interfacial Sliding of Polymer Brushes: a Molecular Dynamics Simulation. *Phys. Rev. Lett.* **1996**, *76* (26), 4979–4982.

(19)   Murat, M.; Grest, G. S. Molecular Dynamics Simulations of the Force Between a Polymer Brush and an AFM Tip. *Macromolecules* **1996**, *29* (25), 8282–8284.

(20) Singh, M. K.; Ilg, P.; Espinosa-Marzal, R. M.; Kröger, M.; Spencer, N. D. Polymer Brushes Under Shear: Molecular Dynamics Simulations Compared to Experiments. *Langmuir* **2015**, *31* (16), 4798–4805.

(21) Galuschko, A.; Spirin, L.; Kreer, T.; Johner, A.; Pastorino, C.; Wittmer, J.; Baschnagel, J. Frictional Forces Between Strongly Compressed, Nonentangled Polymer Brushes: Molecular Dynamics Simulations and Scaling Theory. *Langmuir* **2010**, *26* (9), 6418–6429.

(22) Irfachsyad, D.; Tildesley, D.; Malfreyt, P. Dissipative Particle Dynamics Simulation of Grafted Polymer Brushes Under Shear. *Phys. Chem. Chem. Phys.* **2002**, *4* (13), 3008–3015.

(23) Chen, M.; Briscoe, W. H.; Armes, S. P.; Klein, J. Lubrication at Physiological Pressures by Polyzwitterionic Brushes. *Science* **2009**, *323* (5922), 1698–1701.

(24) Goicochea, A. G.; Mayoral, E.; Klapp, J.; Pastorino, C. Nanotribology of Biopolymer Brushes in Aqueous Solution Using Dissipative Particle Dynamics Simulations: an Application to PEG Covered Liposomes in a Theta Solvent. *Soft Matter* **2014**, *10* (1), 166–174.

(25) Zhang, Z.; Morse, A. J.; Armes, S. P.; Lewis, A. L.; Geoghegan, M.; Leggett, G. J. Effect of Brush Thickness and Solvent Composition on the Friction Force Response of Poly(2-(Methacryloyloxy)Ethylphosphorylcholine) Brushes. *Langmuir* **2011**, *27* (6), 2514–2521.

(26) McNamee, C. E.; Yamamoto, S.; Higashitani, K. Preparation and Characterization of Pure and Mixed Monolayers of Poly(Ethylene Glycol) Brushes Chemically

Adsorbed to Silica Surfaces. *Langmuir* **2007**, *23* (8), 4389–4399.

(27)   Kitano, K.; Inoue, Y.; Matsuno, R.; Takai, M.; Ishihara, K. Nanoscale Evaluation of Lubricity on Well-Defined Polymer Brush Surfaces Using QCM-D and AFM. *Coll. Surf. B* **2008**, *74* (1), 350–357.

(28)   Rosenberg, K. J.; Goren, T.; Crockett, R.; Spencer, N. D. Load-Induced Transitions in the Lubricity of Adsorbed Poly(L-Lysine)- G-Dextran as a Function of Polysaccharide Chain Density. *ACS Appl. Mater. Interf.* **2011**, *3* (8), 3020–3025.

(29)   Singh, M.; Ilg, P.; Espinosa-Marzal, R.; Spencer, N.; Kröger, M. Influence of Chain Stiffness, Grafting Density and Normal Load on the Tribological and Structural Behavior of Polymer Brushes: a Nonequilibrium-Molecular-Dynamics Study. *Polymers* **2016**, *8* (7), 254.

(30)   Goicochea, A. G.; López-Esparza, R.; Altamirano, M. A. B.; Rivera-Paz, E.; Waldo-Mendoza, M. A.; Pérez, E. Friction Coefficient and Viscosity of Polymer Brushes with and Without Free Polymers as Slip Agents. *J Molec. Liq.* **2016**, *219*, 368–376.

(31)   Yamamoto, S.; Ejaz, M.; Tsujii, Y.; Fukuda, T. Surface Interaction Forces of Well-Defined, High-Density Polymer Brushes Studied by Atomic Force Microscopy. 2. Effect of Graft Density. *Macromolecules* **2000**, *33*, 5608–5612.

(32)   Dimitrov, D. I.; Milchev, A.; Binder, K. Polymer Brushes in Solvents of Variable Quality: Molecular Dynamics Simulations Using Explicit Solvent. *J. Chem. Phys.* **2007**, *127* (8), 084905.

(33)   Espinosa-Marzal, R. M.; Nalam, P. C.; Bolisetty, S.; Spencer, N. D. Impact of

Solvation on Equilibrium Conformation of Polymer Brushes in Solvent Mixtures. *Soft Matter* **2013**, *9* (15), 4045.

(34)   Nomura, A.; Okayasu, K.; Ohno, K.; Fukuda, T.; Tsujii, Y. Lubrication Mechanism of Concentrated Polymer Brushes in Solvents: Effect of Solvent Quality and Thereby Swelling State. *Macromolecules* **2011**, *44* (12), 5013–5019.

(35)   Li, A.; Benetti, E. M.; Tranchida, D.; Clasohm, J. N.; Schönherr, H.; Spencer, N. D. Surface-Grafted, Covalently Cross-Linked Hydrogel Brushes with Tunable Interfacial and Bulk Properties. *Macromolecules* **2011**, *44* (13), 5344–5351.

(36)   Gong, J. P. Friction and Lubrication of Hydrogels?Its Richness and Complexity. *Soft Matter* **2006**, *2*, 544.

(37)   Kim, S. H.; Opdahl, A.; Marmo, C.; Somorjai, G. A. AFM and SFG Studies of pHEMA-Based Hydrogel Contact Lens Surfaces in Saline Solution: Adhesion, Friction, and the Presence of Non-Crosslinked Polymer Chains at the Surface. *Biomaterials* **2002**, *23* (7), 1657–1666.

(38)   Pan, Y.-S.; Xiong, D.-S.; Ma, R.-Y. A Study on the Friction Properties of Poly(Vinyl Alcohol) Hydrogel as Articular Cartilage Against Titanium Alloy. *Wear* **2006**, *262* (7), 1021–1025.

(39)   Gong, J. P.; Higa, M.; Iwasaki, Y.; Katsuyama, Y.; Osada, Y. Friction of Gels. *J. Phys. Chem. B* **1997**, *101* (28), 5487–5489.

(40)   Caravia, L.; Dowson, D.; Fisher, J.; Corkhill, P. H.; Tighe, B. J. Friction of Hydrogel and Polyurethane Elastic Layers When Sliding Against Each Other Under a Mixed Lubrication Regime. *Wear* **1995**, *181*, 236–240.

(41)   Gong, J. P.; Kurokawa, T.; Narita, T.; Kagata, G.; Osada, Y.; Nishimura, G.; Kinjo, M. Synthesis of Hydrogels with Extremely Low Surface Friction. *J. Am. Chem. Soc.* **2001**, *123* (23), 5582–5583.

(42)   Mamada, K.; Fridrici, V.; Kosukegawa, H.; Kapsa, P.; Ohta, M. Friction Properties of Poly(Vinyl Alcohol) Hydrogel: Effects of Degree of Polymerization and Saponification Value. *Tribol. Lett.* **2011**, *42* (2), 241–251.

(43)   Lin, S.; Gu, L. Influence of Crosslink Density and Stiffness on Mechanical Properties of Type I Collagen Gel. *Materials* **2015**, *8*, 551–560.

(44)   Julthongpiput, D.; Ahn, H.-S.; Kim, D.-I.; Tsukruk, V. V. Tribological Behavior of Grafted Polymer Gel Nanocoatings. *Tribol. Lett.* **2002**, *13* (1), 35–40.

(45)   Wong, R. S. H.; Ashton, M.; Dodou, K. Effect of Crosslinking Agent Concentration on the Properties of Unmedicated Hydrogels. *Pharmaceutics* **2014**, *7* (3), 305–319.

(46)   Kobayashi, M.; Terada, M.; Takahara, A. Polyelectrolyte Brushes: a Novel Stable Lubrication System in Aqueous Conditions. *Faraday Discuss.* **2012**, *156*, 403–410.

(47)   Zhang, Q.; Archer, L. A. Interfacial Friction and Adhesion of Cross-Linked Polymer Thin Films Swollen with Linear Chains. *Langmuir* **2007**, *23* (14), 7562–7570.

(48)   Kobayashi, M.; Kaido, M.; Suzuki, A.; Takahara, A. Tribological Properties of Cross-Linked Oleophilic Polymer Brushes on Diamond-Like Carbon Films. *Polymer* **2016**, *89*, 128–134.

(49)   Bavaresco, V. P.; Zavaglia, C. A. C.; Reis, M. C.; Gomes, J. R. Study on the Tribological Properties of pHEMA Hydrogels for Use in Artificial Articular Cartilage. *Wear* **2008**, *265* (3-4), 269–277.

(50)   Ohsedo, Y.; Takashina, R.; Gong, J. P.; Osada, Y. Surface Friction of Hydrogels with Well-Defined Polyelectrolyte Brushes. *Langmuir* **2004**, *20* (16), 6549–6555.

(51)   Ishikawa, Y.; Hiratsuka, K.-I.; Sasada, T. Role of Water in the Lubrication of Hydrogel. *Wear* **2005**, *261* (5), 500–504.

(52)   Huang, X. Y.; Wirth, M. J. Surface-Initiated Radical Polymerization on Porous Silica. *Anal. Chem.* **1997**, *69* (22), 4577–4580.

(53)   Hutter, J. L.; Bechhoefer, J. Calibration of Atomic-Force Microscope Tips. *Rev. Sci. Instrum.* **1993**, *64* (7), 1868–1873.

(54)   Sader, J. E.; Chon, J. W. M.; Mulvaney, P. Calibration of Rectangular Atomic Force Microscope Cantilevers. *Rev. Sci. Instrum.* **1999**, *70* (1), 3967–3969.

(55)   Cannara, R. J.; Eglin, M.; Carpick, R. W. Lateral Force Calibration in Atomic Force Microscopy: A New Lateral Force Calibration Method and General Guidelines for Optimization. *Rev. Sci. Instrum.* **2006**, *77* (5) 053701.

(56)   Soddemann, T.; Dünweg, B.; Kremer, K. A Generic Computer Model for Amphiphilic Systems. *Eur. Phys. J. E* **2001**, *6* (5), 409–419.

(57)   Kröger, M.; Loose, W.; Hess, S. Rheology and Structural Changes of Polymer Melts via Nonequilibrium Molecular Dynamics. *J. Rheol.* **1993**, *37* (6), 1057–1079.

(58)   Singh, M. K.; Ilg, P.; Espinosa-Marzal, R. M.; Kröger, M.; Spencer, N. D. Effect of

Crosslinking on the Microtribological Behavior of Model Polymer Brushes. *Tribol. Lett.* **2016**, *63:17,* 1-9.

(59)   Kröger, M. *Models for Polymeric and Anisotropic Liquids;* Berlin Heidelberg, 2005.

(60)   Plimpton, S. Fast Parallel Algorithms for Short-Range Molecular Dynamics. *J. Comput. Phys.* **1995**, *117* (1), 1–19.

(61)   Espinosa-Marzal, R. M.; Bielecki, R. M.; Spencer, N. D. Understanding the Role of Viscous Solvent Confinement in the Tribological Behavior of Polymer Brushes: a Bioinspired Approach. *Soft Matter* **2013**, *9* (44), 10572.

(62)   Simič, R.; Mathis, C. H.; Spencer, N. D. A Two-Step Method for Rate-Dependent Nano-Indentation of Hydrogels. *Polymer* **2018**, *137*, 276–282.

(63)   Klein, J.; Kumacheva, E.; Mahaiu, D.; Perahia, D.; Fetters, L. J. Reduction of Frictional Forces Between Solid Surfaces Bearing Polymer Brushes. *Nature* **1994**, *370* (6491), 634–636.

(64)   Hess, S.; Kröger, M. Elastic and Plastic Behavior of Model Solids. *Techn. Mech.* **2002,** *22*, 79-88.

(65)   Israelachvili, J. N. Intermolecular and Surface Forces; Academic Press: London, 1992.

(66)   Press, W. H.; Flannery, B. P.; Teukolsky, S. A.; Vetterling, W. T. Numerical Recipes in FORTRAN 77: Volume 1, Cambridge University Press, 1992.

ToC Graphic
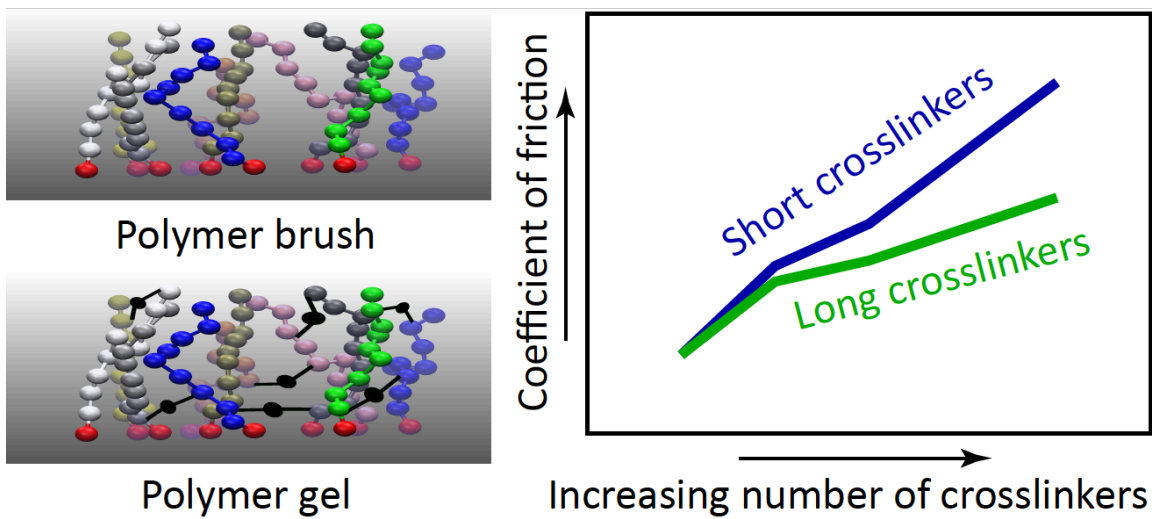
Title:

Combined Experimental and Simulation Studies of Crosslinked Polymer Brushes under Shear

Authors:

Manjesh K. Singh, Chengjun Kang, Patrick Ilg,

Rowena Crockett, Martin Kröger, Nicholas D. Spencer